Hoop fiber and surface matrix strain development on concrete members confined with FRCM composites

Filippo Andreose, Jaime Gonzalez-Libreros, Flora Faleschini, Klajdi Toska, Mariano Angelo Zanini and Carlo Pellegrino

Department of Civil, Environmental and Architectural Engineering, University of Padua, Via Marzolo 9, 35131 Padua, Italy;
Department of Industrial Engineering, University of Padua, Via Gradenigo 6, 35131 Padua, Italy

Abstract
In this paper, the effectiveness of FRCM composites for the confinement of concrete specimens is studied. Concrete cylinders were confined using either carbon- or glass-FRCM jackets, and then tested monotonically under axial load. Performance of the system was evaluated in terms of gain in axial strength and ductility with respect to unconfined specimens. In addition, values of hoop strains recorded with strain gauges mounted on the fibers were compared to those obtained on the composite surface using a digital image correlation (DIC) system. Results show that carbon-FRCM jackets provide higher gain in axial strength than their glass-FRCM counterparts and have a higher fiber exploitation ratio. Measurement of hoop strains on composite surface were significantly higher than those recorded directly on the fibers using strain gauges, for both the FRCM-confinig systems.

1 Introduction
In the previous decade, intensive research has been carried out on the use of fiber reinforced cementitious matrix (FRCM) composites, for improving the flexural, shear, and axial capacity of existing concrete members. FRCM composites are comprised of high strength fibers in the form of open-mesh configuration, and ordinary cement mortars, modified by adding mineral additions (i.e., fly ash or silica fume) and polymers, to improve strength, bond characteristics, durability, and ultimate deformation [1].

Experimental evidences have shown that the use of FRCM composites is able to increase the element strength, although its efficiency is, in general, lower than that achieved by using fiber reinforced polymer (FRP) composites [2]. However, some characteristics of the FRCM system, such as the possibility of applying it on wet surfaces, post-earthquake assessment, and compatibility with the substrate, make them a suitable alternative to the more well-know FRP composites [3].

For the case of axial confinement of concrete members, applying the FRCM jackets along the height of the elements promotes the increase of axial strength and ductility of the confined element with respect to the unconfined case. One of the first studies on this subject [4] analyzed plane concrete cylinders confined with carbon FRCM jackets, which were then tested monotonically under axial load. Results showed that the carbon FRCM jackets were able to attain an increased peak axial strength between 25% and 77%, depending on the applied number of layers and tensile strength of the matrix. The failure mode was characterized by debonding or fiber fracture. The type of failure was attributed as well to different tensile strengths of the mortars used. Although fiber fracture was also reported for FRP confined specimens tested in [4], the FRCM confined elements showed a more ductile failure mode due to a more gradual fracture of the individual fiber bundles.

Garcia et al. [5] confined concrete cylinders using one or two basalt fiber layers, and pozzolanic or Portland cement-based mortars. They witnessed an increase in the axial strength value between 21% and 31%, depending on the mortar type, irrespectively of the number of layers. The highest enhancement was observed for the matrix with the highest tensile strength, that corresponded to the Portland cement-based mortar in this specific case. The failure mode was characterized by the presence of vertical cracks running along the height of the specimen, that widen as the load increased without any fiber fracture. De Caso y Basalo et al. [6] studied the influence of external reinforcement on glass-FRCM confined concrete cylinders. They observed that for the type of system used, the effectiveness of the confinement was not reduced with the number of layers applied; indeed, higher axial strength values were achieved for specimens with the highest number of layers (four in this case). In addition, the failure mode was characterized by the slippage of the fibers in the fiber-matrix interface and partial fiber fracture. Similar results were reported in [7], where PBO-FRCM confined cylinders were experimentally analyzed. Trapko [8], working also with PBO-FRCM confined elements, found that the system was more effective for elements with lower values of unconfined axial strength, i.e., the highest increase in the axial strength value was observed for the members with the lowest unconfined compressive strength.

Colajanni et al. [9] reported an increase in the axial strength and ductility for PBO-FRCM confined concrete elements with square sections, although lower than those of cylinder specimens. For these latter, they found that the increase in axial strength was proportional not only to the number of layers but also to the overlapping length and the mechanical properties of the matrix. Indeed, a higher increase in ductility was observed for those specimens in which a larger value of overlapping length was used.

Ombres and Mazzuca [10], working on a dataset of available experimental tests on FRCM confined specimens, found out that the ratio of confined to unconfined axial strength (f_{cc}/f_{co}) was directly proportional to the axial stiffness of the reinforcement, $\rho_f E_f$, where ρ_f is the confinement reinforcement ratio of the system ($4nt_f/D$ with n=number of fiber layers, t_f=equivalent nominal thickness of the fiber mesh, and D=member diameter), and E_f is the elastic modulus of the bare fibers. They observed also that f_{cc}/f_{co} was inversely proportional to the unconfined axial strength f_{co}.

The above research context highlights that, although several experimental research have been already carried out in this context, there is still need to carry out further efforts to better understand the behavior of such elements, for instance, providing information about the values of strain achieved by the system in the hoop direction. The local evaluation of such strains has been carried out by means of horizontal linear velocity displacement transducers (LVDTs) [11] or strain gauges [12] attached to the matrix surface. However, as pointed out by several researchers [12], failure of the system usually occurs at the matrix-fiber interface and not on the substrate or at the matrix-substrate fiber, as it is usually found for FRP composites. This implies that, for the case of FRCM composites, contrary to the case of FRP composites, strains on the fibers should be determined, instead of on the matrix surface. To evaluate such strains, strain gauges attached to the fiber surface before embedding it in the matrix have been successfully used to study the bond behavior of FRCM composites [13]. More recently, digital image correlation (DIC) systems have also been used to study the behavior of FRCM strengthened concrete and masonry elements [14].

DIC is a non-contact measurement technique that identifies the coordinates of points and patterns in images using imaging sensors [15]. The use of DIC within the civil engineering field has been focused on the measurement of displacements, deflections, and presence of cracks in reinforced concrete (RC) and masonry structures, but also more recently on the study of FRCM-confined members too [16].

In this study, plain concrete cylindrical members were confined using FRCM composites with two different fiber types: carbon and alkali-resistant (AR) glass. The influence of the FRCM system on the behavior of the confined elements was evaluated in terms of increase of axial strength, ductility, and crack development on the composite surface. The FRCM system hoop strains were studied by means of strain gauges mounted on the fibers and compared to those recorded on the matrix surface by means of DIC system. Values of fiber strains recorded were then used to compare predicted and experimental values of lateral confinement pressures and gain in axial strength provided by the FRCM system.

2 Experimental program

Nine specimens of 150 mm of diameter (D) and 300 mm height (H) were included in the experimental campaign presented in this paper. Three specimens worked as control specimens (NC-S3), three were confined (C-S3) with two layers of carbon FRCM composites and the remaining three were confined with two layers of glass-FRCM composite (G-S3). They were realized with a low-strength concrete mixture, having an average compressive strength class target of 15 MPa at 28 days, representing a low-strength, deteriorated concrete situation, that might require retrofit interventions.

The FRCM composite systems used were commercially available from a single producer. Carbon and glass, dry, open mesh textiles were employed. Glass fiber bundles, as delivered by the producer, were coated to improve the bond between the fiber and the matrix. Both the system used for the confinement of the specimens were provided by a single, same, producer. Fiber features are listed in Table 1. Concerning the cementitious matrix, it consisted in a premixed mono-component low modulus fiber-reinforced matrix with polymeric and inorganic binders with pozzolanic property, to be hydrated with water at a water/binder ratio of 0.17. The mechanical characteristics of the matrix, obtained using

40x40x160 mm prisms were: flexural strength (f_{fm}) = 5.3 MPa; and compressive strength (f_{cm}) = 22.9 MPa, both evaluated within 4 days from cylinders testing.

Table 1 Fiber properties.

Fiber type	W (g/m^2)	E_f (GPa)	f_u (MPa)	ε_{fu} (%)	t_f (mm)	ρ_f	$\rho_f E_f$ (GPa)
C (carbon)	170	240	4700	1.8	0.047	0.0025	0.602
G (glass)	251	70	2000	>3.0	0.050	0.0027	0.175

Concerning the strengthening procedure, surface preparation consisted in a superficially damping only. A first layer of matrix was then applied on the wet concrete surface. Immediately after, the first fiber layer was placed on top of the fresh matrix and pressed gently. The fiber layer was then covered by a second matrix layer and the procedure was repeated for the second fiber layer and the third and final matrix layer. Afterwards, the last matrix layer was superficially damped and the specimens were covered by a wet cloth that was removed seven days after the confinement procedure took place. The average thickness of each matrix layer was approximately equal to 4 mm. An overlapping length of 150 mm was used.

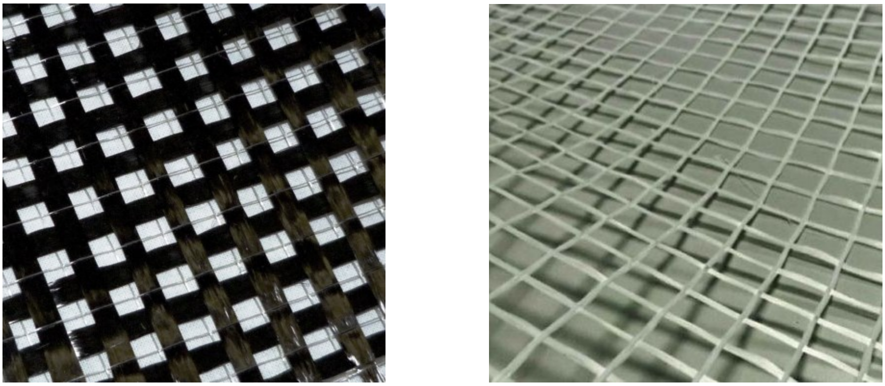

Fig. 1 Carbon (left) and glass (right) mesh configuration.

For the loading protocol, specimens were tested under monotonical axial compression loading using a hydraulic press with a total capacity of 600 kN. A constant displacement rate of 0.6 mm/min was used for testing the specimens. Three LVDTs with a gauge length of 100 mm were mounted on concrete specimen surface, placed at the specimen mid-height, equally spaced radially at 120°, to evaluate the axial strain during the loading. Further two LVDTs were used to evaluate the displacement of the press plate (see Fig.2, left). Such instrumentation was used only for the confined specimens, and it aims to record the axial strains after reaching the peak load, using as gauge length the entire height of the specimen. Concerning the monitoring of fiber hoop strains, on one specimen per type, four strain gauges (SGs) were mounted on the fibers before embedding them in the matrix. Two strain gauges were applied in each layer of fiber, in order to analyze the possible difference in the strain values depending on the location of the fiber layer with respect to the concrete surface (see Fig.2, right).

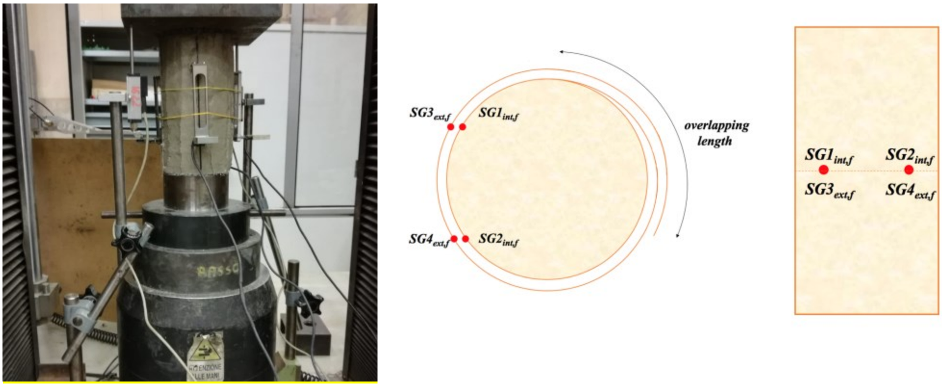

Fig. 2 Test set-up: left, disposition of LVDTs; right, position of strain gauges.

For DIC measurement, a three dimensional (3D) configuration was used in order to avoid significant errors in in-plane displacements, associated with two dimensional (2D) configurations. The stereo-vision system consisted of two monochrome cameras with 5 Megapixel CCD resolution and 12 mm focal length lenses. The two cameras were placed 1.5 m from the samples and oriented with a 36° stereo angle. Light-emitting diode (LED) lamps were located close to the specimens to obtain uniform illumination of the samples during testing. Images were acquired with a frequency of 1 Hz. The system was synchronized with the data acquisition system of the testing machine and images were acquired simultaneously with the applied load. The system was calibrated by capturing several images of a known grid pattern in various poses, including significant rotations about all three axes. Before testing, a white base layer was applied on the specimens' surface and then a black ink marker was used to apply a random speckle pattern. Speckles were around 1 mm diameter and 3-5 pixels in size. Fig. 3 shows the location of the virtual strain gage used to evaluate the matrix strains, compared to the speckle pattern adopted in the two confined specimens.

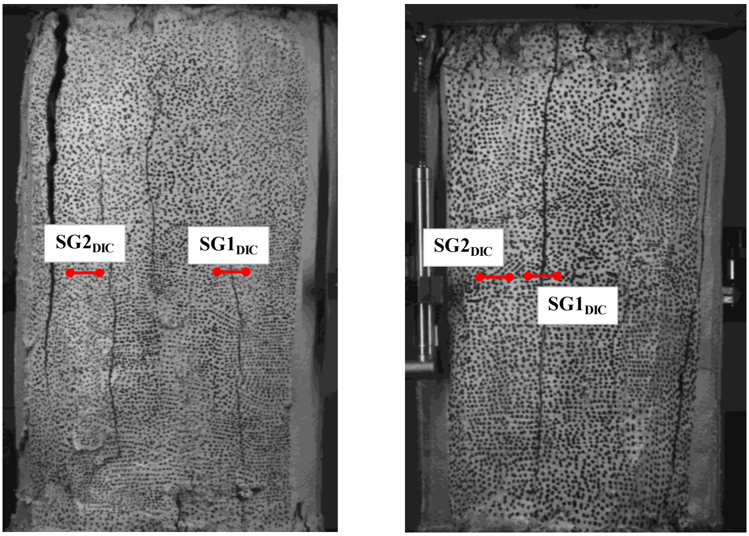

Fig. 3 Location of virtual strain gauges $SG1_{DIC}$ and $SG2_{DIC}$ for specimen: left, C-S3; right, G-S3.

3 Results

3.1 Axial stress vs. axial strain response

Fig. 4 shows the relevant curves plotting the axial stress versus axial strain for the analyzed specimens. In Table 2, instead, average values of peak and ultimate compressive axial strength (f_{co} and $f_{co,u}$, respectively), and peak and ultimate axial strains (ε_{co} and $\varepsilon_{co,u}$, respectively) for unconfined specimens are presented. Table 2 also lists the corresponding average values of confined peak and ultimate compressive axial strengths (f_{cc} and f_{cu}, respectively), and peak and ultimate strains (ε_{cc} and $\varepsilon_{cc,u}$ respectively). In this paper, it was assumed that the ultimate condition of the specimens corresponds to a drop of 15% of the peak load in the post-peak branch of the axial stress vs. axial strain curve. Ratios of confined to unconfined axial strength (f_{cc}/f_{co}), i.e., the increase in the axial strength provided by the FRCM system, of confined or unconfined ultimate axial strength to average peak unconfined axial strength ($f_{co,u}$ or $f_{cc,u}$)/f_{co}, and of ultimate unconfined or confined axial strain to peak unconfined axial strain ($\varepsilon_{co,u}$ or $\varepsilon_{cc,u}$)/ε_{co}, are also shown in Table 2. In one carbon confined specimen a pronounced hardening branch was observed. This resulted in a higher ε_{cc} mean value for the CFRCM series with respect to the glass and non confined ones.

Table 2 Results of the axial behavior.

Series	f_{co} or f_{cc} (MPa)	f_{cc}/f_{co} (-)	$f_{co,u}$ or $f_{cc,u}$ (MPa)	($f_{co,u}$ or $f_{cc,u}$)/f_{co} (-)	ε_{co} or ε_{cc} (%)	$\varepsilon_{co,u}$ or $\varepsilon_{cc,u}$ (%)	($\varepsilon_{co,u}$ or $\varepsilon_{cc,u}$)/ε_{co} (-)
NC-S3	16.8	-	14.3	0.85	0.164	0.272	1.66
C-S3	22.3	1.32	19.0	1.13	0.218	0.905	5.52
G-S3	19.3	1.15	16.4	0.97	0.102	0.407	2.49

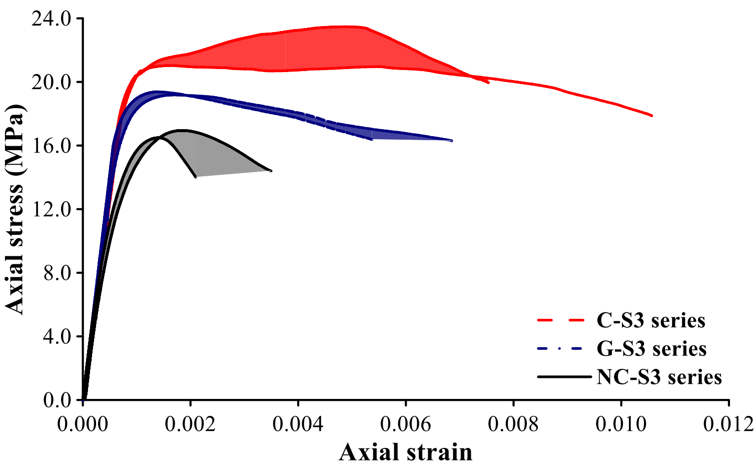

Fig. 4 Envelope of the axial stress vs. axial strain curve for NC-S3, C-S3, and G-S3 series.

3.2 Failure mode of confined specimens and influence of fiber

Failure mode was characterized by vertical cracks on the FRCM jackets running along the height of the specimens. For G-S3 specimens, one of the first vertical cracks appeared around the beginning of the overlapping zone before peak load was attained. As the load increased, original cracks, that formed relatively early, continued growing in length while new cracks started opening. The final cracking pattern was characterized by a homogeneous crack distribution around the perimeter of the specimens. Instead, for C-S3 specimens, formation of cracks was preceded by the concentration of high values of strain on the matrix surface. All specimens, except one, showed a softening post-peak branch which would suggest that specimens failure is due to the slippage of fibers into the matrix. Fig. 5 shows the post test C-S3 (left) and G-S3 (right) specimens.

Fig. 5 Post-test cracking pattern: left, C-S3; right, G-S3.

Results in Fig. 4 and Table 2 show that the FRCM jackets can provide an increase in the axial strength, irrespectively of the type of fiber used. However, the gain in strength for carbon-FRCM confined elements is around two times higher than that observed for glass-FRCM confined specimens, although the area of confinement provided was the same for the two systems. Indeed, the fibers have the same equivalent nominal thickness t_f. However, as expressed before, the effectiveness of the system is not related exclusively to the amount of reinforcement provided but to the system axial rigidity $\rho_f E_f$. As shown in Table 1, carbon-FRCM confined system has a higher value of $\rho_f E_f$ because carbon fibers have a higher elastic modulus than glass fibers, which explains the differences in the gain in axial strength. All specimens except one showed a softening post-peak branch which would suggest that specimens failure is due to the slippage of fibers into the matrix.

FRCM confined specimens show also larger post-peak descending branches with significantly far higher values of ultimate axial strain when compared to that of unconfined elements. The increase in ductility is higher for carbon-FRCM jackets which indicates that this system is more effective than its glass counterpart, as demonstrated by the higher value of $\varepsilon_{cc,u}/\varepsilon_{co}$ reported in Table 2.

3.3 Hoop fibers and matrix strains

For specimen C-S3, Fig.6 (left) shows that strains in carbon fibers start to be recorded and increase rapidly for values of $f_{cc}/f_{cc,max}$ that range between 0.85 and 0.90, independently of the location of the strain gauge (layer or position in the cylinder perimeter). This point coincides with the development of the first longitudinal crack in the matrix surface. For this specimen, the highest values of strain were recorded for the strain gauge mounted on the first fiber layer ($SG1_{int,f}$). For this strain gauge, the maximum value of hoop strain recorded ($\varepsilon_{xx,max}$) was equal to 0.0044, which corresponds to a fiber exploitation ratio ($\varepsilon_{xx,max}/\varepsilon_{fu}$) of 0.25. Lower values of this parameter were obtained for the fibers in the second layer, implying that the first layer is more effective than the second one. For glass confined specimens the first longitudinal cracks in the matrix surface apear for values of $f_{cc}/f_{cc,max}$ between 0.4 and 0.5 which explains the sudden increase of strain in the glass confined series as shown in Fig. 6 (left). This difference from the carbon specimens is due to the higher axial stiffness of the carbon system that guarantees higher confinement with less strain developments. For specimen G-S3, Fig. 6 (right) shows that the higher values of ε_{xx} are recorded for both strain gauges mounted on the external fiber layer. The maximum exploitation value found was equal to 0.17, recorded for strain gauge $SG1_{ext,f}$. which is lower than that found for specimen C-S3-3, although the hoop strain (taken in absolute value) is higher. The higher values of strains recorded on the external layer might be associated with the early matrix cracking and the cracking pattern.

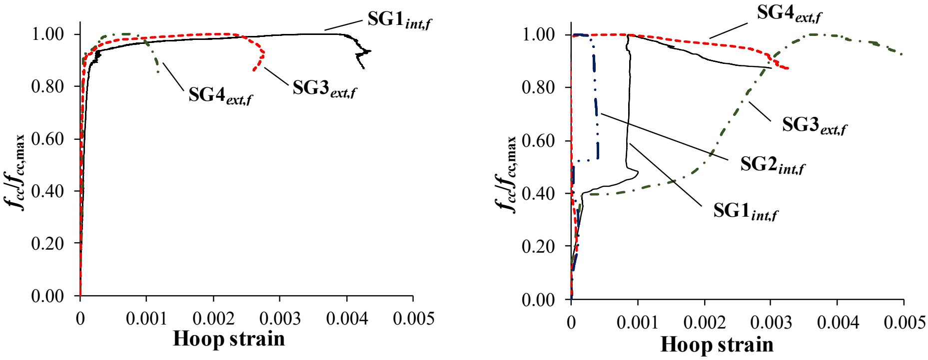

Fig. 6 Normalized axial stress $f_{cc}/f_{cc,max}$ vs. hoop strain for specimens: left, C-S3; right, G-S3.

Lastly, results recorded by virtual strain gage placed in the transverse direction and based on DIC system show that matrix surface strains are considerably higher than those recorded by the strain gauges mounted on the fibers (see Fig. 7 compared to Fig. 6, right-side, for specimen G-S3). These results imply that measurement of strains made on the composite surface can highly overestimate the actual hoop strains developed on the fibers. This mismatch can be easily associated to the cracking pattern development onto the matrix surface.

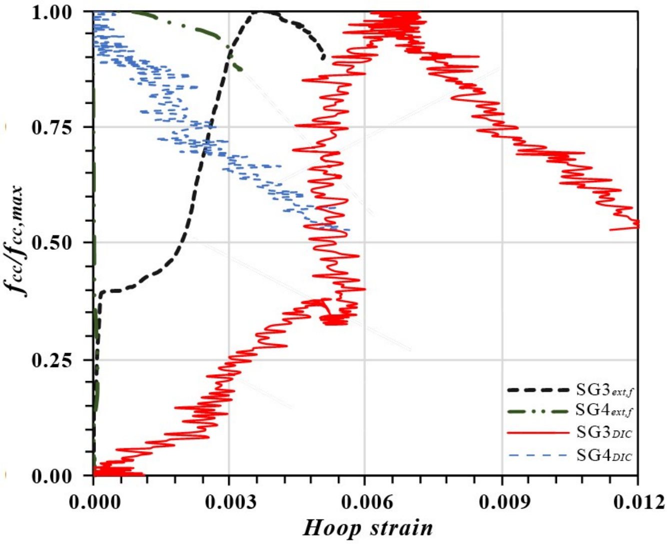

Fig. 7 Normalized axial stress $f_{cc}/f_{cc,max}$ vs. hoop strain on fiber and matrix surface for specimen G-S3.

4 Conclusions

This paper presents the results of an experimental campaign aimed at studying the behavior of concrete members confined with carbon- and glass-FRCM composites. The cracking pattern and evolution of hoop strains measured directly on the fibers and on the surface of the FRCM jacket were also investigated.

The main results proved the effectiveness of FRCM composites to improve the axial strength and ductility of plain concrete specimens confined with FRCM jackets, irrespectively of the type of fibers used. A better performance of the FRCM-system is expected for fibers with higher values of axial stiffness.

Particularly, higher maximum exploitation ratio, i.e., ratio between maximum fiber hoop strain and ultimate fiber strain, was observed for carbon-FRCM confined specimens when compared to their glass-FRCM confined counterparts. In the former specimens, higher values of strain were obtained on the first fiber layer while for the latter members, similar values were recorded for both layers, although higher strains were witnessed on the outer fiber layer.

Lastly, hoop strains measured on the composite surface were significantly higher than those recorded directly on the fibers.

Acknowledgements

Authors would like to acknowledge G&P Intech of Altavilla Vicentina (Italy) for providing the FRCM composite materials.

References

[1] Pellegrino C, D'Antino T 2013. "Experimental behaviour of existing precast prestressed reinforced concrete elements strengthened with cementitious composites." *Compos Part B Eng* 55:31–40.

[2] Tetta ZC, Koutas LN, Bournas DA 2015. "Textile-reinforced mortar (TRM) versus fiber-reinforced polymers (FRP) in shear strengthening of concrete beams." *Compos Part B Eng* 77:338–48.

[3] Triantafillou TC, Papanicolaou CG 2006. "Shear strengthening of reinforced concrete members with textile reinforced mortar (TRM) jackets." *Mater Struct Constr* 39:93–103.

[4] Triantafillou TC, Papanicolaou CG, Zissimopoulos P, Laourdekis T 2006. "Concrete confinement with textile-reinforced mortar jackets." *ACI Struct J* 103:28–37.

[5] García D, Alonso P, San-José J-T, Garmendia L, Perlot C. 2010. "Confinement of medium strength concrete cylinders with basalt Textile Reinforced Mortar." Paper presented at the 13th Int Congr Polym Concr [ICPIC 2010] 0–7.

[6] De Caso Y Basalo FJ, Matta F, Nanni A 2012. "Fiber reinforced cement-based composite system for concrete confinement." *Constr Build Mater* 32:55–65.

[7] Ombres L 2014. "Concrete confinement with a cement based high strength composite material." *Compos Struct* 109:294–304.

[8] Trapko T 2014. "Confined concrete elements with PBO-FRCM composites." *Constr Build Mater* 73:332–8.

[9] Colajanni P, De Domenico F, Recupero A, Spinella N 2014. "Concrete columns confined with fibre reinforced cementitious mortars: Experimentation and modelling." *Constr Build Mater* 52:375–84.

[10] Ombres L, Mazzuca S 2017. "Confined Concrete Elements with Cement-Based Composites : Confinement Effectiveness and Prediction Models."*J Compos Constr* 21:1–15.

[11] Ombres L. "Concrete confinement with a cement based high strength composite material." J *Compos Struct* 2014;109:294–304.

[12] Di Ludovico M, Prota A, Manfredi G. 2010 "Structural Upgrade Using Basalt Fibers for Concrete Confinement." *J Compos Constr* 14:541–52.

[13] D'Antino T, Carloni C, Sneed LH, Pellegrino C. 2014 "Matrix-fiber bond behavior in PBO FRCM composites: A fracture mechanics approach." *Eng Fract Mech* 117:94–111.

[14] Cascardi A, Micelli F, Aiello MA. 2018 "FRCM-confined masonry columns: experimental investigation on the effect of the inorganic matrix properties." *Constr Build Mater* 186:811–25.

[15] Sabau, C., Popescu, C., Sas, G., Blanksvärd, T. and Täljsten, B. (2018) "Axially Loaded RC Walls with Cutout Openings Strengthened with FRCM Composites", *J Compos Constr* 22(6): 1–16. doi: 10.1061/(ASCE)CC.1943-5614.0000867.

[16] Gonzalez J, Zanini MA, Faleschini F, Pellegrino C. (2019) "Confinement of low-strength concrete with fiber-reinforced cemntitious matrix (FRCM) composites" *Comp Part B: Eng,* doi: 10.1061/j.compositesb.2019.107.107407.